ADVANCED ENGINEERING MATERIALS
www.aem-journal.com

Check for updates

# Laser-Triggered Degradation of Silicon Circuits by Lithiation and Moisture Uptake for On-Demand Transient Electronics

Shengnan Liu, Xibo Wang, Shangbin Liu, Yuping Deng, Bochen Zhao, Huachun Wang, Xing Sheng, Lingyun Zhao, Liu Wang,* Peijian Zhang,* and Lan Yin*

**Data security risks of unauthorized access of confidential information have attracted considerable attention. Transient electronics capable of physical disappearance or disintegration upon external stimuli could potentially offer an alternative solution at the device level. Despite great advances, smart, efficient, wireless, and nonrecoverable degradation of foundry-compatible silicon (Si)-integrated circuit (IC) chips remains a challenge. Herein, a laser-triggered degradation of Si circuits by lithiation and moisture uptake is proposed. By integrating IC chips with a small amount of lithium sources and a fluidic reservoir consisting of hygroscopic materials, on-demand, wireless, rapid, and complete degradation of Si IC chips built at 600 nm node is achieved upon activation by laser irradiation. This work paves a new route to accomplish smart, tether-free, and thorough degradation of devices compatible with existing foundry processes, offering an essential baseline for the development of intelligent transient electronics for secured hardware.**

## 1. Introduction

Electronic systems play a critical role in consumer electronics, biomedicine, business infrastructure, internet of things (IoT), etc.[1] Data security concerns with unauthorized access of financial and personal information through cyberattacks, electronic viruses, and device theft have been attracting great attention.[2] Transient electronics represents an emerging type of device that could provide alternative solutions to conventional methods such as software encryption, in the sense that electronic platforms are capable of physical transience including vanishing and shattering in response to external triggering stimuli, which could potentially eliminate information leakage at hardware level under unexpected emergencies.[3]

Various stimuli have been proposed to trigger on-demand degradation, including water,[4] moisture,[5] heat,[6] light,[7] electricity,[8] etc. Most reported works have been focused on the degradation of relatively simple devices such as metallic interconnects and low-density arrays of transistors; however, the triggered degradation of integrated silicon (Si) circuits remains daunting due to the chemically inert nature in near-neutral aqueous environments of silicon and silicon oxide that serve as the basic materials of information technology.[5a,9] To achieve rapid transient functions, strong alkaline substances (e.g., sodium hydroxide (KOH)), hazardous acid (e.g., hydrofluoric acid (HF)), or elevated temperature are often involved to accelerate the degradation process. Strategies including chemical, thermal, and electrical triggering have been proposed to achieve on-demand degradation of Si integrated circuits (ICs). For example, thermally triggered outflow of chemical etchants and thermal activation of energetic films have been shown to realize the damage of

S. Liu, X. Wang, S. Liu, Y. Deng, B. Zhao, L. Zhao, L. Yin
School of Materials Science and Engineering
The Key Laboratory of Advanced Materials of Ministry of Education
State Key Laboratory of New Ceramics and Fine Processing
Center for Flexible Electronics Technology
Tsinghua University
Beijing 100084, P. R. China
E-mail: lanyin@tsinghua.edu.cn

H. Wang, X. Sheng
Department of Electronic Engineering
Beijing National Research Center for Information Science and Technology
Institute for Precision Medicine, Center for Flexible Electronics Technology, and IDG/McGovern Institute for Brain Research
Tsinghua University
Beijing 100084, China

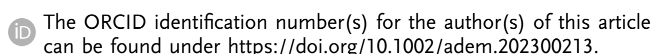
The ORCID identification number(s) for the author(s) of this article can be found under https://doi.org/10.1002/adem.202300213.

DOI: 10.1002/adem.202300213

L. Wang
Key Laboratory of Biomechanics and Mechanobiology of Ministry of Education
Beijing Advanced Innovation Center for Biomedical Engineering
School of Biological Science and Medical Engineering, And with the School of Engineering Medicine
Beihang University
Beijing 100083, P. R. China
E-mail: liuwang@buaa.edu.cn

P. Zhang
National Key Laboratory of Integrated Circuits and Microsystems
Sichuan Institute of Solid-state Circuits
Chongqing 400060, China
E-mail: pjzhang@whu.edu.cn

 © 2023 Wiley-VCH GmbH

15272648, 2023, 12, Downloaded from https://onlinelibrary.wiley.com/doi/10.1002/adem.202300213 by Tsinghua University Library, Wiley Online Library on [26/06/2023]. See the Terms and Conditions (https://onlinelibrary.wiley.com/terms-and-conditions) on Wiley Online Library for rules of use; OA articles are governed by the applicable Creative Commons License

Si chips.[6h,j,8a] Extensive research has been conducted to investigate the interactions between lithium and silicon electrodes in battery applications, with the aim of increasing battery capacity. Studies on electrochemical cracking phenomena of amorphous silicon by lithiation and[10] lithium transformation of monocrystalline silicon and deformation stresses[11] have confirmed that the insertion of Li ions into Si leads to significant volume change[8d,12] and causes electrode cracking, which pose a major challenge to the cycling life of silicon anode lithium batteries. Such a lithiation-induced cracking phenomenon could be harnessed to realize on-demand accelerated Si degradation for transient electronics. Our previous work has demonstrated the feasibility to achieve electrochemically triggered transience of thin-film Si circuits by lithiation. Complete and irreversible degradation of Si circuits based on electrochemical lithiation has been demonstrated.[8d] Despite great progress, further advanced strategies are needed to achieve rapid, wireless, and thorough degradation of foundry-compatible integrated Si electronics.

Here, we propose a laser-triggered complete degradation of Si ICs with irreversible failure through lithiation and moisture uptake (**Figure 1**). By combining Si chip with a small amount of lithium (Li) source, rapid cracking and function failure within 8 s is achieved with laser as a wireless heating source. Prelithiation of Si circuits before laser triggering can realize more thorough degradation while not compromise device performance, due to the formation of extensive microcracks which is confined in the handle layer of Si chips. The integration of Si chip with a fluidic reservoir enables simultaneous laser-induced moisture uptake, accomplishing subsequent complete degradation of lithiated Si chips with alkaline solutions within 5 min. This work provides new avenues toward wireless, rapid, unrecoverable, and on-demand degradation of integrated Si circuits compatible with existing Si manufacturing process, enabling critical material strategies and device schemes to achieve intelligent transient electronics.

## 2. Results and Discussion

### 2.1. Materials Strategies of Triggered Degradation of Si Circuit

The materials and layout of triggered degradation of integrated Si electronics by lithiation and moisture uptake are shown in Figure 1. Specifically, the platform includes: 1) a fluidic reservoir containing hygroscopic materials (superabsorbent polymer [SAP, polyacrylate] and KOH) encapsulated by a phase change material (tetradecyl alcohol); 2) an integrated Si circuit; and 3) a thin lithium foil as the lithiation source (Figure 1a). Upon the application of near-infrared laser, lithium source rapidly becomes molten and cracks the Si circuit within 8 s (Figure 1b). The time required for destruction is highly influenced by the speed at which lithium melts. Therefore, higher power levels and shorter distances result in shorter trigger times and better degradation effects. The relationship between laser power and melting time of Li with an interaction distance at 2 cm is given in Figure S3, Supporting Information. Prelithiated Si circuit can introduce more severe cracking of the Si circuit which will be discussed later. The exposure to laser simultaneously triggers the phase transformation of the encapsulation layer of tetradecyl alcohol in the fluidic reservoir and enables moisture uptake through hygroscopic materials (Figure 1c). The resulting alkaline fluids subsequently flow out and react with the shattered Si circuit (within 5 min), and thorough and nonrecoverable degradation of Si IC can therefore be achieved. The influence of prelithiation, laser-induced cracking, and moisture uptake on the degradation of Si circuits will be discussed in the following sections.

### 2.2. Prelithiation of Si Circuit

Although laser-triggered melting of lithium source can rapidly crack Si due to liquid metal embrittlement,[13] the resulting fragments often have relatively large sizes, which could be subjected to potential recovery (Figure S1, Supporting Information). In contrast, prelithiation can introduce additional microcracks in Si circuits in advance and achieve a more thorough degradation upon laser irradiation and subsequent water degradation. The schematic illustration of thermal prelithiation is shown in **Figure 2**a. Thermal annealing of silicon-on-insulator (SOI)-based integrated Si circuits with the back side of Si handle layer (≈135 μm) in contact with lithium source at elevated temperature (120 °C, 20 h) introduces the formation of $Li_xSi$ alloy and vein-like microcracks, and subsequent reactions with water accelerate the degradation of Si circuits (Figure 2a).

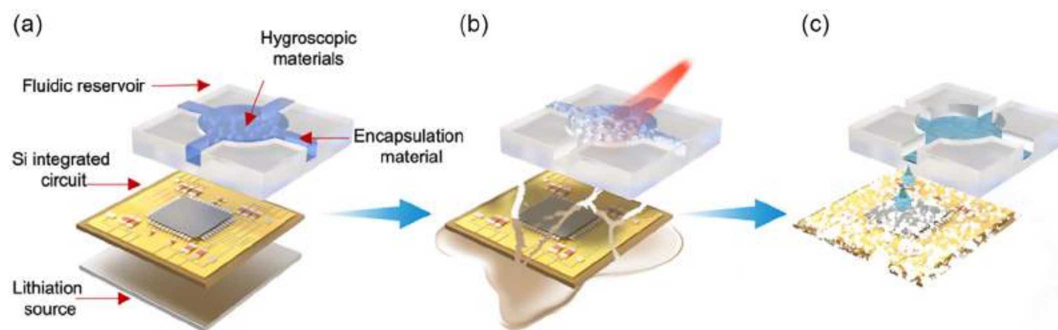


**Figure 1.** Laser-triggered degradation of IC by lithiation and moisture uptake for on-demand transient electronics. a) Layouts of the laser-triggered transient platform, consisting of a fluidic reservoir encapsulating hygroscopic materials by a phase change material (tetradecyl alcohol) and a lithiation source. b) Laser triggers the melting of the phase change material and the cracking of Si IC by melted lithium. Prelithiated Si circuit induces more thorough cracking. c) Melting of the encapsulation material leads to moisture uptake by the hygroscopic materials in the fluidic reservoir. The resulting outflow of water induces further degradation of Si IC and achieves a nonrecoverable circuit destruction.

 © 2023 Wiley-VCH GmbH

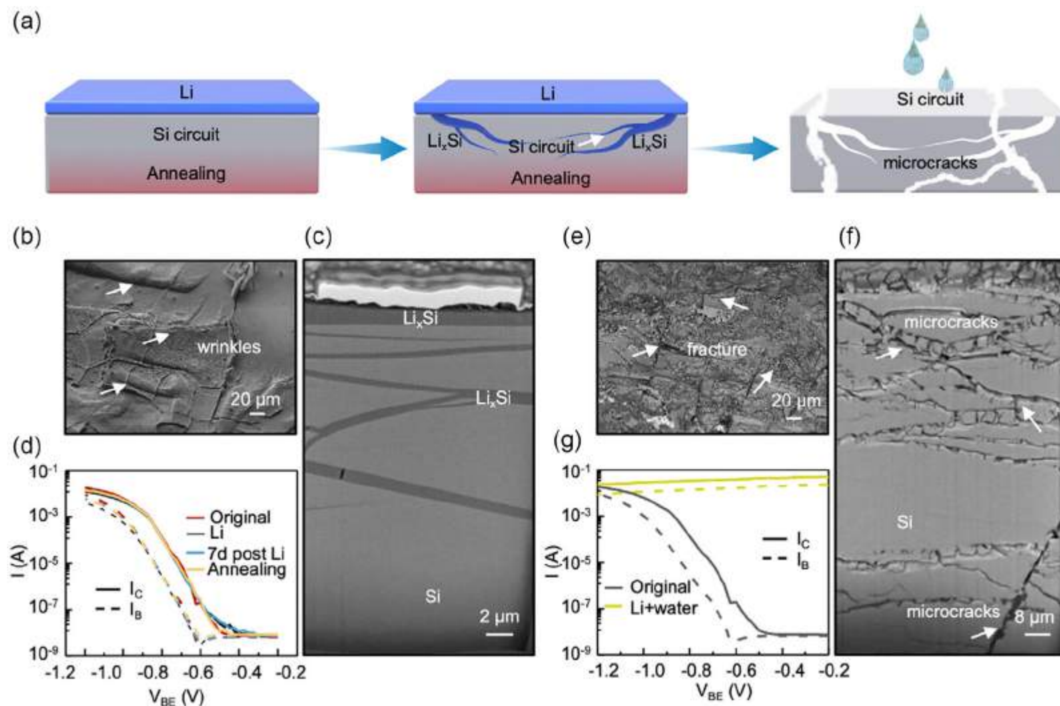


**Figure 2.** Thermal prelithiation of Si circuit. a) Schematic illustration of thermal prelithiation followed by water degradation. Annealing at elevated temperature with lithium source introduces the formation of $Li_xSi$ alloy and vein-like microcracks in Si. The addition of water accelerates subsequent degradation of Si circuit. b) Surface morphology of the back side of the handle layer of the Si circuit after thermal prelithiation. c) Cross-sectional view of the Si circuit after thermal prelithiation (light grey area: Si, dark grey area: $Li_xSi$ alloy). d) Electrical performance of the BJT device before (original) and after (Li) prelithiation at 120 °C for 20 h, room-temperature storage of 7 days after prelithiation (7d post-Li), and annealing at 120 °C for 20 h without lithiation (Annealing). e) Surface morphology of prelithiated Si circuit after the addition of water. f) Cross-sectional view of the prelithiated Si circuit after the addition of water. g) Electrical performance of the BJT device before prelithiation (original) and after prelithiation and water degradation (Li + water).

The surface of the back side of the Si handle layer and the cross-sectional microstructure of Si samples are investigated by a focused ion beam–scanning electron microscope (FIB–SEM) and the results are shown in Figure 2b,c. The buckling surface morphology is attributed to the residual stress due to lithiation. A planar $Li_xSi$ layer (≈1.5 μm) is found on the outer layer of the sample, with a deep vein-like network of $Li_xSi$ layer (≈17 μm), consistent with the previous reported microstructure of electrochemically lithiated Si samples.[8d,14] Microcracks are associated with lithiated regions and can provide fast paths for Li diffusion to greatly enhance Li-affected zones and ultimately accelerate the degradation of Si.[14a] Auger electron spectroscopy (AES) is carried out on the surface of a prelithiated Si sample. The depth profile is achieved through argon (Ar) sputtering (Figure S2, Supporting Information). The result confirms the presence of $Li_xSi$ alloy in prelithiated sample, consistent with previous reports.[8d] We identify the darker region of the FIB–SEM image as $Li_xSi$ alloy and the lighter region as unreacted monocrystalline silicon (Figure 2c). The Gummel–Poon (G–P) curves of high-speed bipolar junction transistors (BJTs) on the IC chip before prelithiation (original), after prelithiation at 120 °C for 20 h (Li), storage at room temperature in low-oxygen environment of 7 days after prelithiation (7d post-Li), and annealing at 120 °C for 20 h without lithiation (annealing) are given in Figure 2d. Interestingly, the results show no significant difference in the high-voltage region ($V_{BE} < -0.6$ V), suggesting the device performance is not compromised by prelithiation under current conditions likely due to the relatively thick Si handle layer (≈135 μm) and the presence of the buried oxide layer (≈1 μm) which blocks Li diffusion as reported in a previous work.[15]

The current prelithiation treatment involves subjecting the device to 120 °C for 20 h, resulting in a Li-affected zone of ≈17 μm (Figure 2c) and subsequent degradation of SOI-based Si circuits of 150 μm. One possible strategy for shortening the prelithiation time is to thin the handle layer of the SOI device, resulting in a thinner required Li-affected zone that could potentially reduce the required prelithiation time. Further investigations are needed to identify optimized prelithiation conditions for Si chips with different thicknesses.

With the addition of water droplets (≈0.5 mL) on the surface of the thermally prelithiated Si circuit, rapid reactions with $Li_xSi$ occur and the associated stress can even lead to macroscopic cracking in some samples. The surface and cross-sectional morphology of prelithiated Si circuits after the reaction with water is shown in Figure 2e,f. Microcracks are observed both on the surface and in the vein-like $Li_xSi$ layer which was extended to a much deeper region (≈40 μm). The loss of electrical functions of BJTs on the device layer after the addition of water is observed, probably due to the intense reaction and the formation of extensive

 © 2023 Wiley-VCH GmbH

15272648, 2023, 12, Downloaded from https://onlinelibrary.wiley.com/doi/10.1002/adem.202300213 by Tsinghua University Library, Wiley Online Library on [26/06/2023]. See the Terms and Conditions (https://onlinelibrary.wiley.com/terms-and-conditions) on Wiley Online Library for rules of use; OA articles are governed by the applicable Creative Commons License

15272648, 2023, 12, Downloaded from https://onlinelibrary.wiley.com/doi/10.1002/adem.202300213 by Tsinghua University Library, Wiley Online Library on [26/06/2023]. See the Terms and Conditions (https://onlinelibrary.wiley.com/terms-and-conditions) on Wiley Online Library for rules of use; OA articles are governed by the applicable Creative Commons License

microcracks (Figure 2g). The short-circuit failure mode may be caused by water and Li penetration that shorts the device. The results suggest that thermal prelithiation could introduce sufficient microcracks and residual stress in a convenient manner compared with the previously reported electrochemical method,[8d] enabling subsequent thorough degradation while not compromising the performance of SOI-based Si circuits on the device layer.

### 2.3. Laser-Triggered Degradation of Prelithiated Si Circuit

**Figure 3**a presents the schematic illustration of laser-triggered degradation of a prelithiated Si device. The laser is considered as a wireless and convenient heating source that enables rapid, localized, and on-demand triggering of the degradation of integrated Si circuits. In comparison, hot plates or furnaces can also function as heat sources, but they are relatively bulky, requiring devices to be tethered to specific locations, and heating speed is relatively slow. In addition, laser heating has a more precise and controllable spatial resolution, making it suitable for use with miniaturized Si circuits. The primary objective of using the laser in the current work is to wirelessly generate heat and achieve a molten lithium source. This, in turn, enables the cracking of the Si circuit (within 8 s), resulting in the formation of an additional $Li_xSi$ alloy, as well as microcracks and macroscopic cracking. We utilized an 808 nm near-infrared laser because it is a common light source for photothermal heating experiments and can achieve rapid heating. While high-energy photons could cause functional failure of Si circuits,[16] we focused on utilizing the heat effects of the laser to achieve complete physical transience of the Si chip. The presence of residual stress, extensive vein-like $Li_xSi$ alloy, and microcracks in the Si handle layer resulting from prelithiation make the Si circuit more vulnerable to laser-triggered degradation as greatly enhanced pathways are available for molten Li to penetrate and crack Si circuit, which also ensure subsequent complete degradation upon the addition of water.

Various stages of laser-triggered degradation of a prelithiated Si circuit are shown in Figure 3b. Laser triggers quick melting of Li and enables the cracking of Si circuit by molten Li (within 8 s) which simultaneously penetrate through microcracks resulting

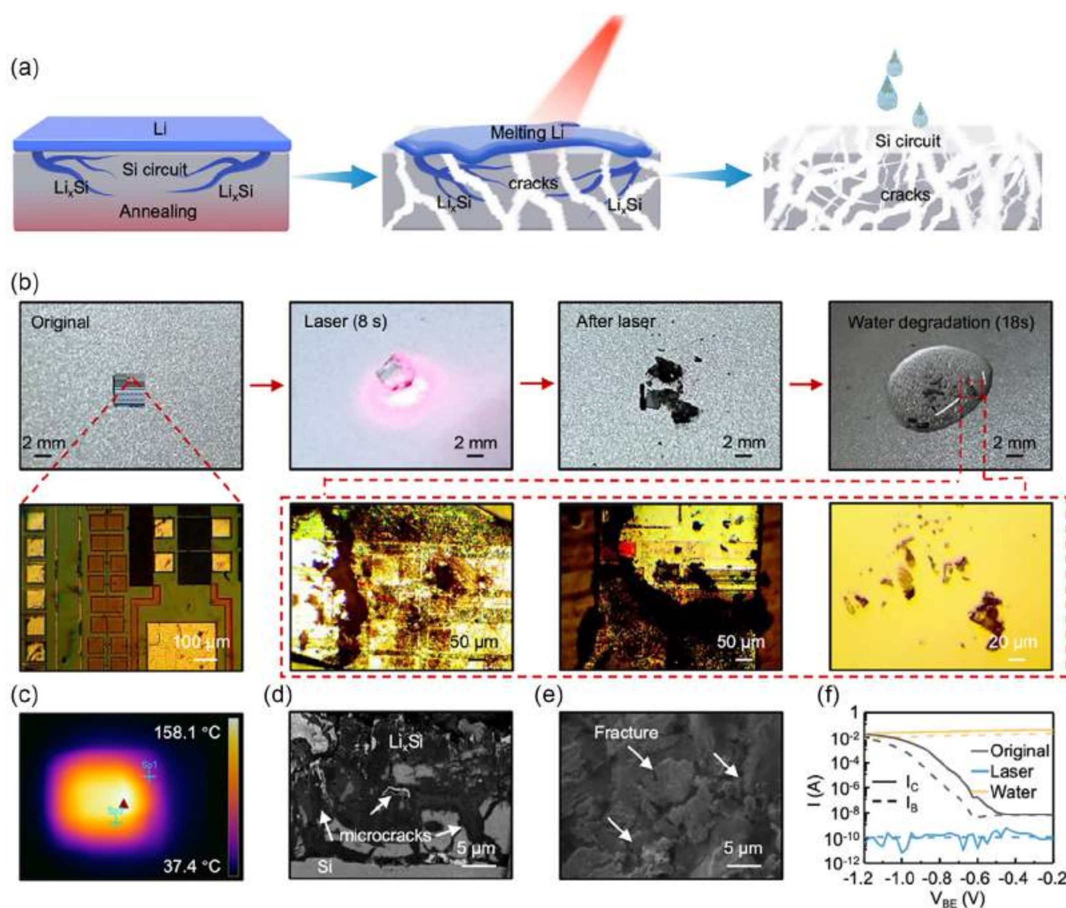


**Figure 3.** Laser-triggered degradation of a prelithiated Si circuit. a) Schematic illustration of laser-triggered cracking of a prelithiated Si circuit. Laser triggers the melting of lithiation source and introduces the formation of additional $Li_xSi$ alloy and microcracks as well as macroscopic cracking. The addition of water leads to complete degradation of a Si circuit. b) Various stages of laser-triggered degradation of a prelithiated Si circuit followed by water degradation. c) Infrared image during the course of laser-triggered degradation. d) Cross-sectional view of a Si circuit after laser-triggered degradation (light grey area: Si, dark grey area: $Li_xSi$ alloy). e) Surface morphology of a Si circuit after laser-triggered degradation. f) Electrical performance of the original BJT device (Original), after prelithiation and laser-triggered degradation (Laser), and after water degradation (Water).


© 2023 Wiley-VCH GmbH

from prelithiation to achieve severe fracturing and the extensive formation of $Li_xSi$ alloy. The addition of water further assists complete degradation of Si circuit into tiny and nonrecoverable pieces (Figure 3b). In contrast, laser-triggered degradation of Si circuit without prelithiation cracks within 8 s further degrades into fragments through subsequent water degradation. But the resulting fragments are relatively large and degradation is less thorough compared to prelithiated silicon circuits, probably due to the absence of microcracks and a vein-like network of $Li_xSi$ alloy in the handle layer of the device (Figure S4, Supporting Information). The thermal infrared image during the course of laser triggering indicates that the temperature of Li approaches close to its melting point (180.5 °C) (Figure 3c). The cross-sectional and surface morphology after laser irradiation reveal severe cracking and the formation of extensive $Li_xSi$ regions which is critical to realize a thorough transience of Si circuit (Figure 3b,e). The electrical performance of original BJTs (Original), after prelithiation, and laser-triggered degradation (Laser) and after degradation in water (Water) is shown in Figure 3f. Two failure modes of BJTs are observed. The short circuit is likely caused by water or Li penetration that shorts the device, whereas open-circuit failure is probably due to cracking that breaks electrical connections. Since we are testing severely damaged residual fragments, these two failure modes occur randomly. These results suggest that the combination of prelithiation, laser triggering, and water degradation can achieve rapid and complete fracturing of Si circuits.

### 2.4. Moisture Uptake of Hygroscopic Materials in the Fluidic Reservoir

As water source is essential to further assist complete degradation of Si circuit after laser irradiation, a fluidic reservoir capable of moisture uptake by laser triggering is developed, and the schematic illustration shows in **Figure 4**a. The fluidic reservoir consists of a customized chamber with 4 outlets, hygroscopic materials (SAP and KOH), and an encapsulation layer made of a phase-change material (tetradecyl alcohol, ≈300 μm). Moisture uptake is activated by laser-induced melting of the encapsulation layer at temperatures slightly above 39 °C, which exposes the hygroscopic materials in ambient atmosphere. The formation and outflow of alkaline solutions resulting from SAP and KOH provide the water source for the degradation of Si circuits. The process of moisture uptake triggered by laser is given in Figure 4b, and the hygroscopic materials are dyed with red pigment to facilitate visualization. The moisture uptake process from the ambient environment is also shown in Movie S1, Supporting Information. The results demonstrate that laser irradiation (≈8 s) can rapidly trigger the melting of the sealing layer (≈1 min) and the outflow of liquid can be achieved within 5 min through moisture uptake from air under normal humidity.

To investigate the influence of alkaline solutions formed by moisture uptake on Si degradation rates, pattered monocrystalline Si thin films on SOI wafers are achieved (Figure S5, Supporting Information). The degradation process of pattered Si thin films (5 μm) induced by moisture uptake of hygroscopic materials at 40 °C is shown in Figure 4c. The averaged Si degradation rates in alkaline solutions obtained by moisture uptake as a function of relative humidity (RH) at 25 °C are given in Figure 4d, indicating that a humid environment facilitates a faster degradation rate.

The moisture uptake over time of KOH, SAP, and the combination of KOH and SAP (KOH/SAP ratio of 5:1) is given in Figure 4e and S6, Supporting Information. KOH serves as the main hygroscopic component and is competent of rapid moisture uptake, while SAP assists the retention of absorbed water. As the concentration of alkaline solutions plays an important role in the degradation rates of Si, the calculated KOH concentrations based on water absorption after 1 h are summarized in Figure 4f. Humid environment (90% RH, 25 °C) gives rise to lower KOH concentrations (≈30 wt%) than those obtained with 30%RH (≈50 wt%) because of more water absorption, while slightly elevated temperature (40 °C) results in similar KOH concentrations as those obtained at 25 °C. Si degradation rates with lower KOH concentrations obtained with 90%RH are expected to be greater than those with higher KOH concentrations obtained with 30% RH, according to the previously reports that the fastest Si dissolution has been observed with KOH solutions around 18 wt% and either increase or decrease in KOH concentrations results in decreased dissolution rates.[17] These results again support that a humid environment promotes Si degradation rates.

The influence KOH-to-SAP ratios is also investigated as a function of RH, and the results are given in Figure S7, Supporting Information. With a greater humidity (90%RH), a higher KOH/SAP ratio (e.g., 10:1) corresponds to greater degradation rates probably due to rapid moisture uptake and proper KOH concentrations. In contrast, the higher proportion of SAP is preferred with low humidity (30%RH) to ensure sufficient retention of absorbed water, as evaporation could become significant due to less water absorption. An intermediate level of KOH/SAP ratio of 5:1 is therefore chosen to adapt to a wider range of humidity. Moreover, Si with greater doping levels yields lower degradation rates which are consistent with reported rates (Figure S8, Supporting Information).[18] These results offer material strategies to optimize hygroscopic materials supplying alkaline solutions for rapid degradation of Si circuits.

### 2.5. Laser-Triggered Complete Degradation of Integrated Si Circuit

An SOI-based IC chip (150 μm thickness) fabricated by foundry-compatible complementary bipolar technology is used to demonstrate laser-triggered transience through lithiation and moisture uptake. The chip is cut into a rectangle with a size of 4 × 1.8 mm. The representative structure of the chip is presented in **Figure 5**a. The corresponding thicknesses of the passivation layer (PV) consisting of insulating oxides ($SiO_2$ and silicon nitride ($Si_3N_4$)), device layer (Si), and buried oxides ($SiO_2$) are 1, 13, and 1 μm, respectively. The IC chip is prelithiated at 120 °C for 20 h and assembled with the aforementioned fluidic reservoir with a tiny Li thin foil placed beneath the chip (Figure 5b). After the laser irradiation is switched on for 8 s, the IC chip cracks quickly and the encapsulation layer of the fluidic reservoir simultaneously melts after about 1 min, exposing hygroscopic materials to the ambient atmosphere. Bubbles are visible in the reservoir during the course of the formation of alkaline solution due to moisture


© 2023 Wiley-VCH GmbH

15272648, 2023, 12, Downloaded from https://onlinelibrary.wiley.com/doi/10.1002/adem.202300213 by Tsinghua University Library, Wiley Online Library on [26/06/2023]. See the Terms and Conditions (https://onlinelibrary.wiley.com/terms-and-conditions) on Wiley Online Library for rules of use; OA articles are governed by the applicable Creative Commons License

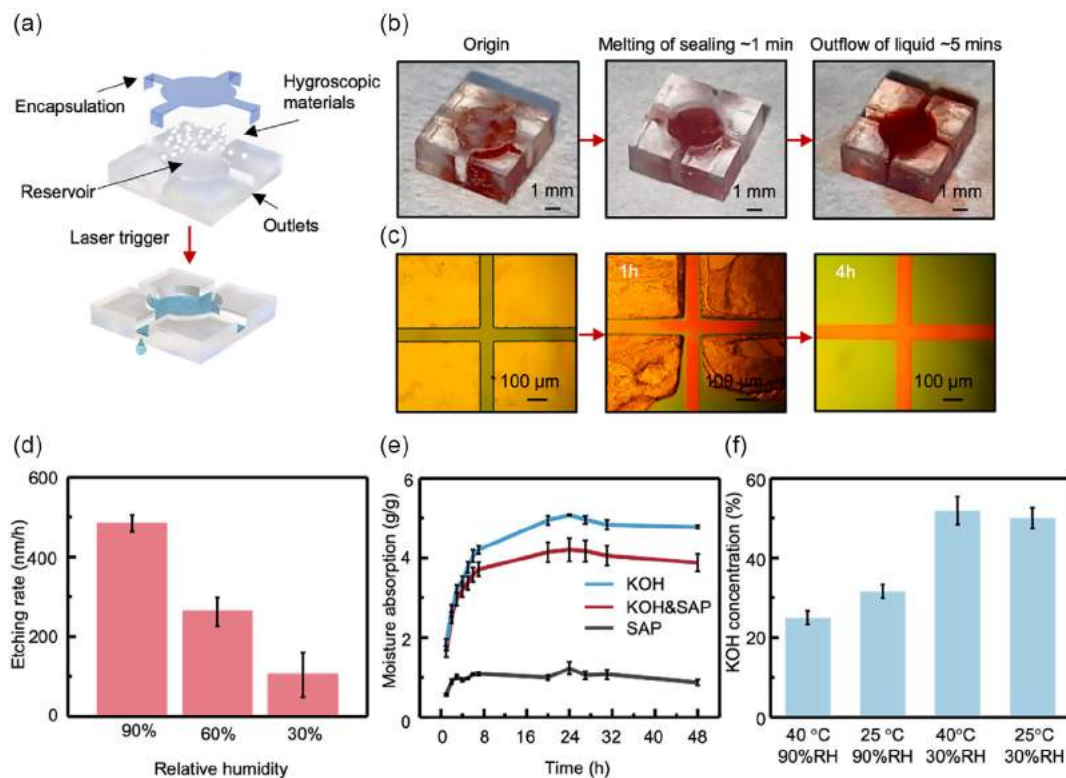


**Figure 4.** Moisture uptake of hygroscopic materials in the fluidic reservoir. a) Schematic illustration of laser-triggered moisture uptake. The fluidic reservoir consists of a customized chamber with four outlets, hygroscopic materials (SAP), and an encapsulation layer made of a phase change material (tetradecyl alcohol, ≈300 µm). Laser triggers melting of the encapsulation layer followed by moisture uptake of the hygroscopic materials, forming alkaline solutions for subsequent circuit degradation. b) Optical images of various stages of moisture uptake. c) Optical images of the degradation process of pattered monocrystalline Si triggered by moisture uptake of the hygroscopic materials. d) Averaged degradation rates of monocrystalline Si under different humidity at 25 °C. e) Moisture absorption of hygroscopic materials (KOH/SAP = 5:1) at 25 °C in air with 90% RH. f) Resulting KOH concentrations after moisture uptake of 1 h at different temperatures and RH.

uptake. The outflow of liquid is observed after around 5 min, and the reaction with $Li_xSi$ and remaining Si component lead to further degradation of the IC chip into nonrecoverable fragments (Figure 5b). The time elapse images of the degradation process of the IC chip are shown in Figure 5c. Within 8 s of laser triggering, the IC chip fractures into small pieces with severely damaged surfaces, and subsequent degradation with absorbed water enables further thorough degradation into the debris. The laser-triggered degradation process of the Si IC chip is given in Movie S2, Supporting Information. These results demonstrate that on-demand, irreversible, and complete degradation of IC chips can be accomplished by laser-triggered lithiation and moisture uptake.

## 3. Discussion

Herein, we propose a wireless, rapid, and complete laser-triggered degradation of Si IC chips by lithiation and moisture uptake. By introducing a small amount of Li source to IC chips, laser-induced heat quickly triggers the melting of Li and achieves liquid metal-induced shattering within 8 s. Prelithiation results in the formation of more extensive microcracks and enables significantly greater pathways for liquid Li penetration, contributing to a more thorough degradation. Integration with a fluidic reservoir with hygroscopic materials, moisture uptake is simultaneously activated along with laser-induced cracking. The absorption of water realizes the acquisition of alkaline etchants and allows subsequent reaction with lithiated IC chips, enabling further complete degradation. Compared with the previously reported method (Table S1, Supporting Information), the strategy in the current work accomplishes wireless, rapid, and thorough degradation of foundry-compatible Si IC chips. The end products are mostly $Li_xSi$ alloys and debris, minimizing the chance of chip recovery. Additionally, the management of electronic waste (E-waste) has become a major challenge for human society. Landfills are commonly used for disposing of E-waste, but there is increasing attention being given to recycling electronics.[19] While the proposed devices aim to be applied to secured hardware, they could also be used to reduce E-waste such as Si chips and minimize environmental impact. As the end-products mainly consist of small amount of $Li_xSi$ and debris, Si chips can easily degrade in the environment through exposure to water or rain, thereby reducing the need for landfill space and potentially saving costs and labor associated with recycling. In all, this work offers new strategies to achieve on-demand, rapid, and thorough

 © 2023 Wiley-VCH GmbH

15272648, 2023, 12, Downloaded from https://onlinelibrary.wiley.com/doi/10.1002/adem.202300213 by Tsinghua University Library, Wiley Online Library on [26/06/2023]. See the Terms and Conditions (https://onlinelibrary.wiley.com/terms-and-conditions) on Wiley Online Library for rules of use; OA articles are governed by the applicable Creative Commons License

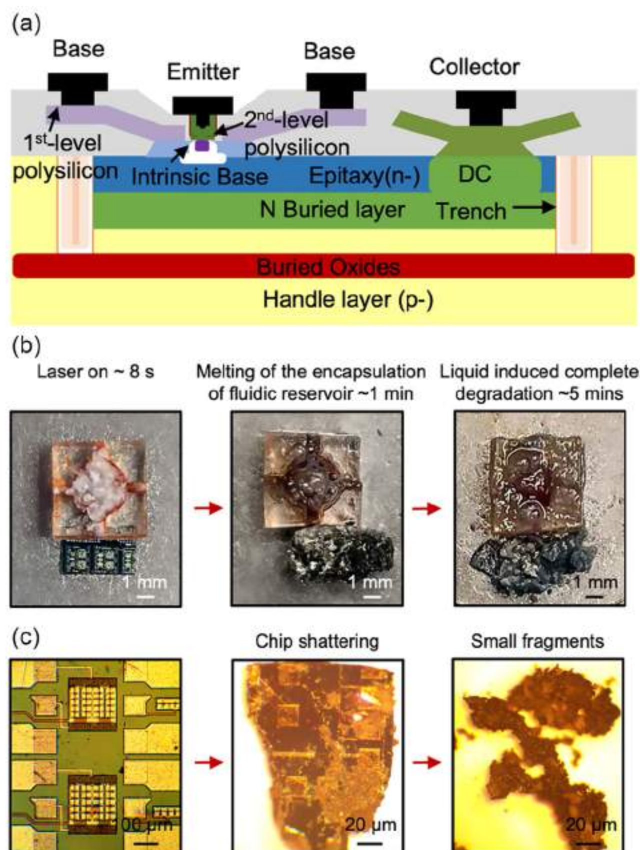


**Figure 5.** Complete degradation of integrated Si circuit triggered by laser. a) Schematic illustration of SOI-based Si circuit with BJT devices. b) Photos of the degradation process triggered by laser irradiation. c) Optical images of Si circuit at various stages of laser-triggered on-demand degradation.

degradation of IC chips compatible with foundry manufacturing in a wireless manner, providing important engineering basis for the development of intelligent transient electronics that could be beneficial for data security.

## 4. Experimental Section

*Thermal Prelithiation of Si circuit*: Prelithiation was achieved by placing thin Li foils (≈ 0.6 mm) on the back sides of Si samples (including 200 μm monocrystal silicon wafer, patterned SOI wafer, and 150 μm Si IC chips) in the alumina crucible at 120 °C for 20 h in the glove box.

*Fabrication of Patterned Monocrystalline Si Membranes*: Patterned monocrystalline Si membranes were achieved based on SOI wafers with different doping levels: low doping level, 5 μm top Si, p-type <100>, 6–8 Ω cm (LIJINGKEJI, Inc.); medium doping level, 3 μm top Si, p-type <100>, 0.277 Ω cm (China electronics technology group); high doping level, 4.5 μm top Si, p-type <100>, 0.01–0.025 Ω cm (LIJINGKEJI, Inc). In most cases, SOI wafers with low doping level (6–8 Ω cm) were adopted as samples unless otherwise specified. SOI wafers were cut into samples with the size of 1 × 1 cm. The top Si layer was patterned in to arrays of squares ($a = 1$ mm) by photolithography with SPR220 photoresist and reactive ion etching (RIE, $SF_6$, 150 sccm, 88 mTorr).

*Fabrication of Fluidic Reservoir with Hygroscopic Materials*: The fluidic reservoir was obtained by laser cutting polymethyl methacrylate (PMMA) into a shape of 5 × 5 × 2 mm, with a cylindrical reservoir ($d = 3$ mm, $h = 1.8$ mm) and four outlets ($w = 1$ mm; $h = 1.8$ mm). The hygroscopic materials were prepared by grinding and mixing KOH powders and SAP (polyacrylate) with a mass ratio of 5:1. The hygroscopic material was then loaded into the reservoir of the fluidic reservoir. The phase change material (tetradecyl alcohol) was applied to the reservoir and outlet at 40 °C and formed a stable encapsulation layer on the hydroscopic materials after rapid cooling to room temperature.

*Laser-Triggered Degradation, Material Characterization, and Electrical Measurements*: The near-infrared laser (808 nm, circle beam with 5 mm diameter) was generated by a semiconductor laser system (GSCLS–05–7W00, Beijing Daheng Photoelectric Technology Co., LTD). The emission and termination of the laser were controlled by a separate switch. The output power of the laser could be increased from 0.5 to 7 W via the control panel. The beam was a circular shape with a diameter of 5 mm at a distance of 2 cm from the light source and beam size increased with distance. The IC chips were high-speed polysilicon emitter bipolar transistors (PE-BJTs) from a 0.6 μm commercial complementary bipolar technology with a minimum breakdown voltage between collector and emitter with the base open ($BV_{CEO}$) of 30 V and a typical value of 4 GHz cutoff frequency. The lithiated or laser-triggered degraded Si samples were washed with diethyl carbonate (DEC) and dried for 5 min. These samples were transferred into the FIB–SEM system (Crossbeam 340, Carl Zeiss, Inc.) by an airtight container to avoid exposure to ambient air. Prior to FIB milling, platinum (1 μm) was deposited on top of the regions of interest to minimize damage of the samples. FIB milling was implemented at 30 kV/300 pA for rough raster and further polished at 30 kV/30 pA at the final step. Surface morphology characterization was performed by an SEM system (JSM-6700F, JEOL Ltd.). The lithiated Si samples were transferred to the AES system (PHI-700, ULVAC-PHI, Inc.) in a sealed vessel to prevent exposure to ambient air. The analysis was carried out at 10 kV. The energy resolution was low as 1‰ and the vacuum in the analysis chamber was better than $3.9 \times 10^{-9}$ Torr. The depth profiles of AES were obtained via argon sputtering with a sputtering rate of 19 nm per minute for the standard sample ($SiO_2$). For the in situ observation of Si circuit during the degradation process, the optical images were taken by a stereomicroscope (Interface 1000E, Gamry Ltd.) and a digital camera (Nikon, DS-U3). To evaluate moisture uptake and degradation characteristics, hygroscopic materials or Si samples with hygroscopic materials were placed in a furnace with a certain temperature and RH. The absorbed water content was weighed as a function of time. The height profile during the process of degradation of patterned monocrystalline Si was monitored by a step profiler (Tencor D-500, KLA) and corresponding averaged degradation rates were calculated over a time frame of 4 h. The electrical performance of the Si chips was measured by Keithley 4200 (Tektronix).

## Supporting Information

Supporting Information is available from the Wiley Online Library or from the author.

## Acknowledgements

The project was supported by the National Natural Science Foundation of China (T2122010 and 52171239 to L.Y., 52272277 to X.S.) and Beijing Municipal Natural Science Foundation (Z220015).

## Conflict of Interest

The authors declare no conflict of interest.

## Data Availability Statement

The data that support the findings of this study are available in the supplementary material of this article.


© 2023 Wiley-VCH GmbH

15272648, 2023, 12, Downloaded from https://onlinelibrary.wiley.com/doi/10.1002/adem.202300213 by Tsinghua University Library, Wiley Online Library on [26/06/2023]. See the Terms and Conditions (https://onlinelibrary.wiley.com/terms-and-conditions) on Wiley Online Library for rules of use; OA articles are governed by the applicable Creative Commons License

15272648, 2023, 12, Downloaded from https://onlinelibrary.wiley.com/doi/10.1002/adem.202300213 by Tsinghua University Library, Wiley Online Library on [26/06/2023]. See the Terms and Conditions (https://onlinelibrary.wiley.com/terms-and-conditions) on Wiley Online Library for rules of use; OA articles are governed by the applicable Creative Commons License

## Keywords

laser triggered, lithiation, on-demand degradation, silicon circuits, transient electronics

Received: February 15, 2023
Revised: April 3, 2023
Published online: May 5, 2023

[1] a) N. Banerjee, Y. Xie, M. M. Rahman, H. Kim, C. H. Mastrangelo, presented at *27th IEEE International Conference on Micro Electro Mechanical Systems (MEMS)*, IEEE, San Francisco, CA, 2014 January; b) S. S. Pandey, C. H. Mastrangelo, presented at *12th IEEE Sensors Conference*, IEEE, Baltimore, MD, 2013 November.

[2] N. Banerjee, Y. Xie, H. Kim, C. H. Mastrangelo, presented at *12th IEEE Sensors Conf.*, IEEE, Baltimore, MD, 2013 November.

[3] a) C. You, H. Zhao, Q. Guo, Y. Mei, *Mrs Bull.* **2020**, *45*, 129; b) G. Lee, Y. S. Choi, H.-J. Yoon, J. A. Rogers, *Matter* **2020**, *3*, 1031; c) J.-S. Shim, J. A. Rogers, S.-K. Kang, *Mater. Sci. Eng. R-Rep.* **2021**, *145*, 100624.

[4] J. W. Shin, J. C. Choe, J. H. Lee, W. B. Han, T. M. Jang, G. J. Ko, S. M. Yang, Y. G. Kim, J. Joo, B. H. Lim, E. Park, S. W. Hwang, *Acs Nano* **2021**, *15*, 19310.

[5] a) A. Douglas, N. Muralidharan, R. Carter, K. Share, C. L. Pint, *Nanoscale* **2016**, *8*, 7384; b) Y. Gao, Y. Zhang, X. Wang, K. Sim, J. Liu, J. Chen, X. Feng, H. Xu, C. Yu, *Sci. Adv.* **2017**, *3*.

[6] a) A. Gumus, A. Alam, A. M. Hussain, K. Mishra, I. Wicaksono, G. A. T. Sevilla, S. F. Shaikh, M. Diaz, S. Velling, M. T. Ghoneim, S. M. Ahmed, M. M. Hussain, *Adv. Mater. Technol.* **2017**, *2*, 1600264; b) G. Li, E. Song, G. Huang, Q. Guo, F. Ma, B. Zhou, Y. Mei, *Adv. Funct. Mater.* **2018**, *28*, 1870323; c) B. H. Kim, J.-H. Kim, L. Persano, S.-W. Hwang, S. Lee, J. Lee, Y. Yu, Y. Kang, S. M. Won, J. Koo, Y. K. Cho, G. Hur, A. Banks, J.-K. Song, P. Won, Y. M. Song, K.-I. Jang, D. Kang, C. H. Lee, D. Pisignano, J. A. Rogers, *Adv. Funct. Mater.* **2017**, *27*, 1870323; d) V. Gund, A. Ruyack, K. Camera, S. Ardanuc, C. Ober, A. Lal, presented at *29th IEEE International Conference on Micro Electro Mechanical Systems (MEMS)*, IEEE, Shanghai, 2016 January; e) E. R. Westphal, A. K. Murray, M. P. McConnell, T. J. Fleck, G. T. C. Chiu, J. F. Rhoads, I. E. Gunduz, S. F. Son, *Propellants Explos. Pyrotech.* **2019**, *44*, 47; f) T. J. Fleck, R. Ramachandran, A. K. Murray, W. A. Novotny, G. T. C. Chiu, I. E. Gunduz, S. F. Son, J. F. Rhoads, *Propellants Explos. Pyrotech.* **2017**, *42*, 579; g) S. K. Lazarouk, A. V. Dolbik, P. V. Jaguiro, V. A. Labunov, V. E. Borisenko, *Semiconductors* **2005**, *39*, 881; h) C. H. Lee, J. W. Jeong, Y. H. Liu, Y. H. Zhang, Y. Shi, S. K. Kang, J. Kim, J. S. Kim, N. Y. Lee, B. H. Kim, K. I. Jang, L. Yin, M. K. Kim, A. Banks, U. Paik, Y. G. Huang, J. A. Rogers, *Adv. Funct. Mater.* **2015**, *25*, 1338; i) G. Li, E. Song, G. Huang, R. Pan, Q. Guo, F. Ma, B. Zhou, Z. Di, Y. Mei, *Small* **2018**, *14*, 1802985; j) X. Ma, S. Gu, Y. Li, J. Lu, G. Yang, K. Zhang, *Adv. Funct. Mater.* **2021**, *31*, 2103199.

[7] H. L. Hernandez, S.-K. Kang, O. P. Lee, S.-W. Hwang, J. A. Kaitz, B. Inci, C. W. Park, S. Chung, N. R. Sottos, J. S. Moore, J. A. Rogers, S. R. White, *Adv. Mater.* **2014**, *26*, 7637.

[8] a) S. S. Pandey, N. Banerjee, Y. Xie, C. H. Mastrangelo, *Adv. Mater. Technol.* **2018**, *3*, 1800044; b) J. Koo, S. B. Kim, Y. S. Choi, Z. Xie, A. J. Bandodkar, J. Khalifeh, Y. Yan, H. Kim, M. K. Pezhouh, K. Doty, G. Lee, Y.-Y. Chen, S. M. Lee, D. D'Andrea, K. Jung, K. Lee, K. Li, S. Jo, H. Wang, J.-H. Kim, J. Kim, S.-G. Choi, W. J. Jang, Y. S. Oh, I. Park, S. S. Kwak, J.-H. Park, D. Hong, X. Feng, C.-H. Lee, A. Banks, C. Leal, H. M. Lee, Y. Huang, C. K. Franz, W. Z. Ray, M. MacEwan, S.-K. Kang, J. A. Rogers, *Sci. Adv.* **2020**, *6*; c) K. Sim, X. Wang, Y. Li, C. Linghu, Y. Gao, J. Song, C. Yu, *J. Micromech. Microeng.* **2017**, *27*, 065010; d) Y. Chen, H. Wang, Y. Zhang, R. Li, C. Chen, H. Zhang, S. Tang, S. Liu, X. Chen, H. Wu, R. Lv, X. Sheng, P. Zhang, S. Wang, L. Yin, *Nanotechnology* **2019**, *30*, 394002.

[9] a) K. M. Lee, E. E. Al, *Cheminform* **2014**, *45*; b) S.-W. Hwang, G. Park, C. Edwards, E. A. Corbin, S.-K. Kang, H. Cheng, J.-K. Song, J.-H. Kim, S. Yu, J. Ng, J. E. Lee, J. Kim, C. Yee, B. Bhaduri, Y. Su, F. G. Omennetto, Y. Huang, R. Bashir, L. Goddard, G. Popescu, K.-M. Lee, J. A. Rogers, *ACS Nano* **2014**, *8*, 5843; c) Y. K. Lee, K. J. Yu, E. Song, A. B. Farimani, F. Vitale, Z. Xie, Y. Yoon, Y. Kim, A. Richardson, H. Luan, *Acs Nano* **2017**, *11*, 12562; d) L. Yin, A. B. Farimani, K. Min, N. Vishal, J. Lam, Y. K. Lee, N. R. Aluru, J. A. Rogers, *Adv. Mater.* **2015**, *27*, 1857; e) L. Wang, Y. Gao, F. Dai, D. Kong, H. Wang, P. Sun, Z. Shi, X. Sheng, B. Xu, L. Yin, *ACS Appl. Mater. Interfaces* **2019**, *11*, 18013.

[10] J. P. Maranchi, A. F. Hepp, A. G. Evans, N. T. Nuhfer, P. N. Kumta, *J. Electrochem. Soc.* **2006**, *153*, A1246.

[11] M. J. Chon, V. A. Sethuraman, A. McCormick, V. Srinivasan, P. R. Guduru, *Phys. Rev. Lett.* **2011**, *107*.

[12] L. Y. Beaulieu, K. W. Eberman, R. L. Turner, L. J. Krause, J. R. Dahn, *Electrochem. Solid-State Lett.* **2001**, *4*, A137.

[13] T. Yoneoka, S. Tanaka, T. Terai, *Mater. Trans.* **2001**, *42*, 1019.

[14] a) S. C. Yong, M. Pharr, S. K. Chan, S. B. Son, S. C. Kim, K. B. Kim, H. Roh, S. H. Lee, K. H. Oh, J. J. Vlassak, *J. Power Sources* **2014**, *265*, 160; b) M. J. Chon, V. A. Sethuraman, A. Mccormick, V. Srinivasan, P. R. Guduru, *Phys. Rev. Lett.* **2011**, *107*, 045503.

[15] a) X. Gao, W. Lu, J. Xu, *Acs Appl. Mater. Interfaces* **2021**, *13*, 21362; b) Z. Liu, Q. Yu, Y. Zhao, R. He, M. Xu, S. Feng, S. Li, L. Zhou, L. Mai, *Chem. Soc. Rev.* **2019**, *48*, 285; c) Y. Zhang, Y. Li, Z. Wang, K. Zhao, *Nano Lett.* **2014**, *14*, 7161.

[16] a) S. K. Tripathi, *Defect Diffus. Forum.* **2013**, *341*, 181; b) M. Caussanel, A. Canals, S. K. Dixit, M. J. Beck, A. D. Touboul, R. D. Schrimpf, D. M. Fleetwood, S. T. Pantelides, *IEEE Trans. Nucl. Sci.* **2007**, *54*, 1925.

[17] H. Seidel, L. Csepregi, A. Heuberger, H. Baumgartel, *J. Electrochem. Soc.* **1990**, *137*, 3612.

[18] H. Seidel, L. Csepregi, A. Heuberger, H. Baumgartel, *J. Electrochem. Soc.* **1990**, *137*, 3626.

[19] K. Zhang, J. L. Schnoor, E. Y. Zeng, *Environ. Sci. Technol.* **2012**, *46*, 10861.


© 2023 Wiley-VCH GmbH

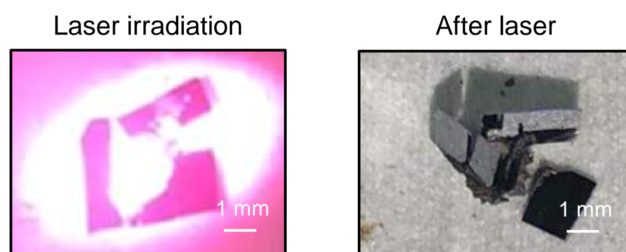


**Figure S1. Images of monocrystalline Si (200 μm) without pre-lithiation during and after laser triggered cracking by the molten lithium source.**

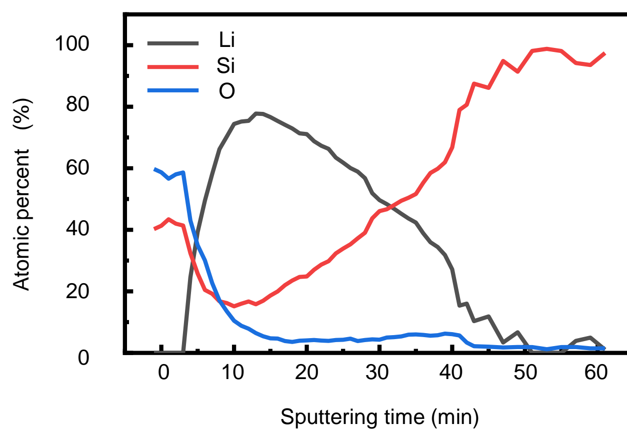


**Figure S2. Auger depth profiles of Li, Si and O of a region on the surface of a pre-lithiated Si sample.**

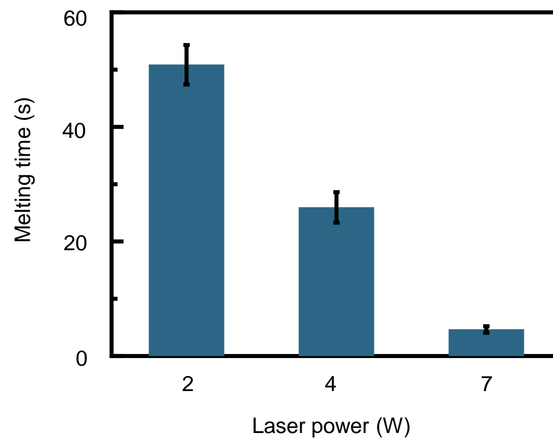


**Figure S3. Influence of different laser power on the melting time of Li. The distance between the light source and the Li source is fixed at 2 cm and the beam has a circular shape with a diameter of 5 mm.**

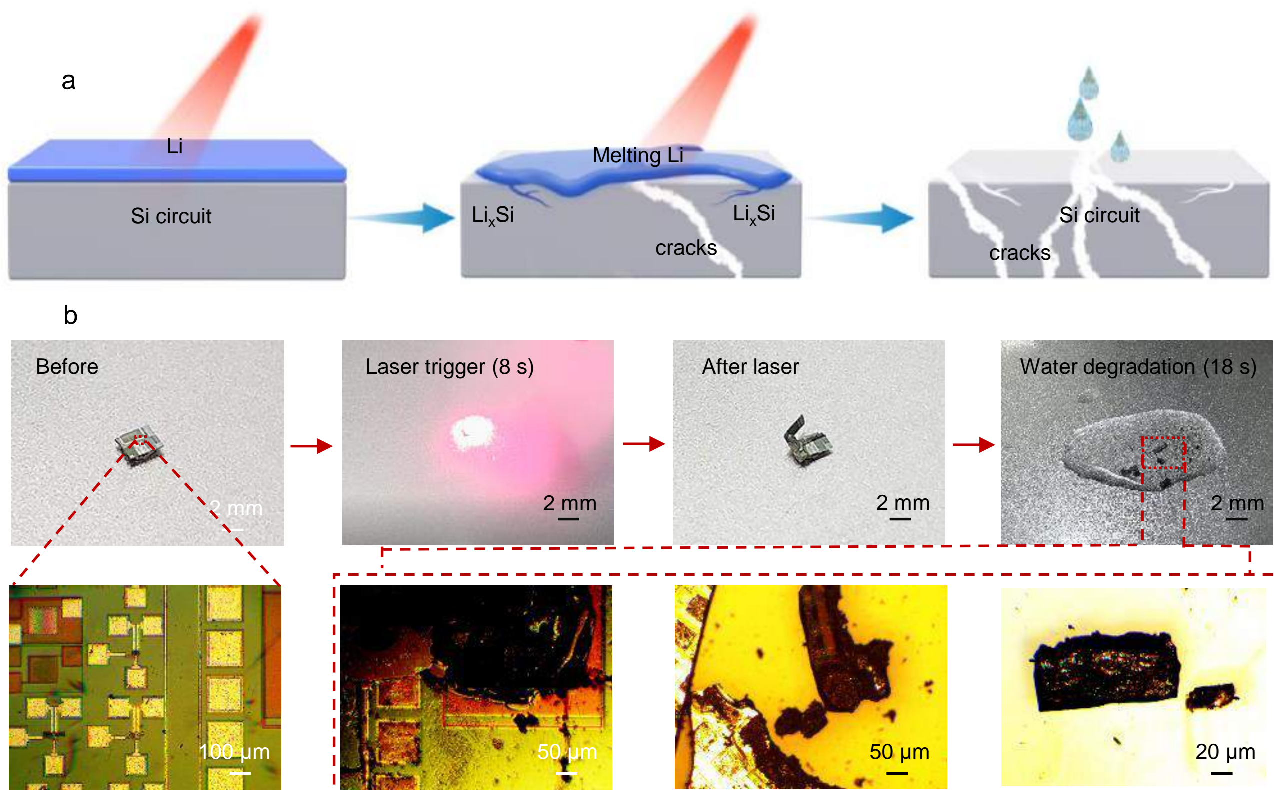


**Figure S4. Laser-triggered degradation of Si circuit without pre-lithiation. a.** Schematic illustration of laser triggered cracking of a Si circuit without pre-lithiation. Laser triggers the melting of lithiation source and introduces the formation of a small amount of $Li_xSi$ alloy and microcracks as well as macroscopic cracking. The addition of water leads to cracking of Si circuit into larger pieces. **b.** Various stages of laser triggered degradation of a Si circuit without pre-lithiation.

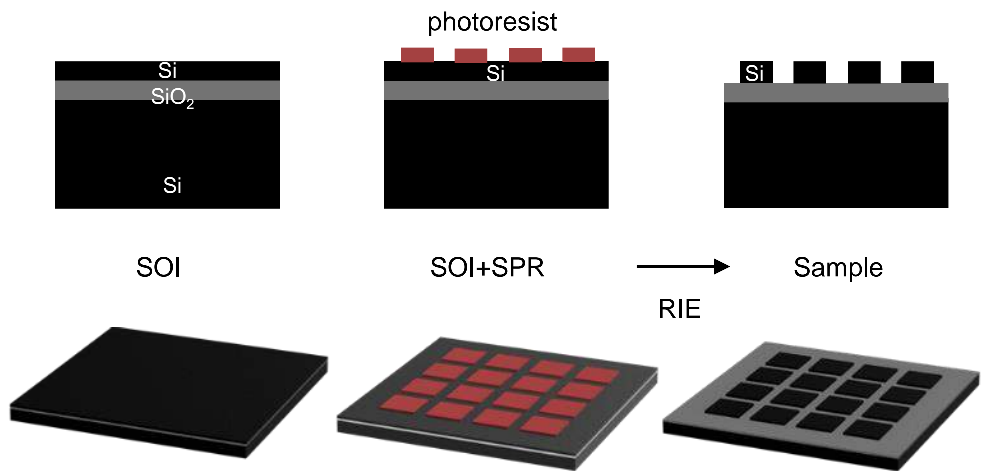


**Figure S5. Fabrication process of monocrystalline silicon patterns on SOI wafers.**

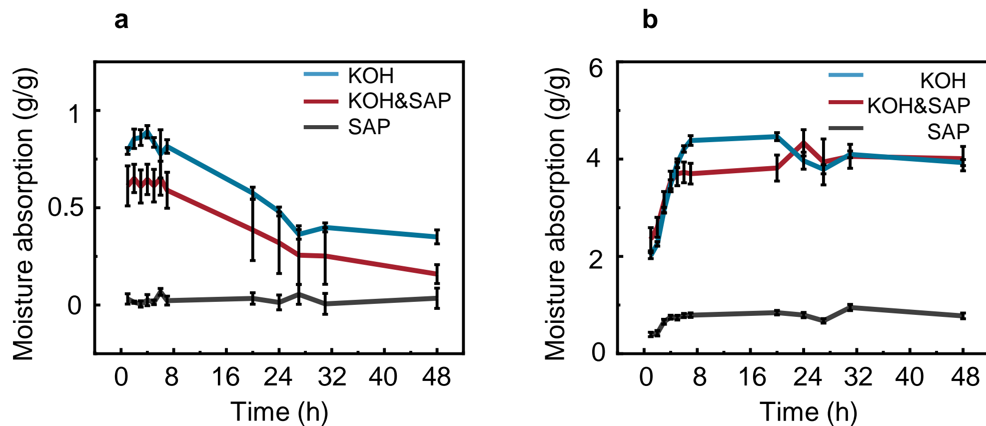


**Figure S6. Moisture uptake as a function of time (KOH/SAP=5:1). a.** 30% RH at 40 $^{o}$C. **b.** 90% RH at 40 $^{o}$C.

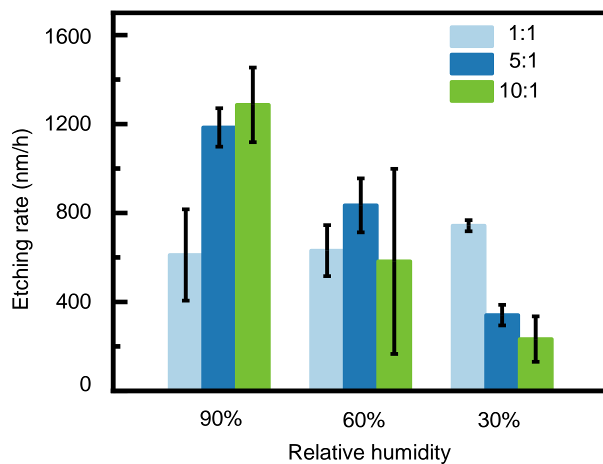


**Figure S7. Si degradation rates resulting from moisture uptake as a function of the composition of hygroscopic materials at 40 °C, with a ratio of KOH/SAP= 1:1, 5:1 and 10:1.**

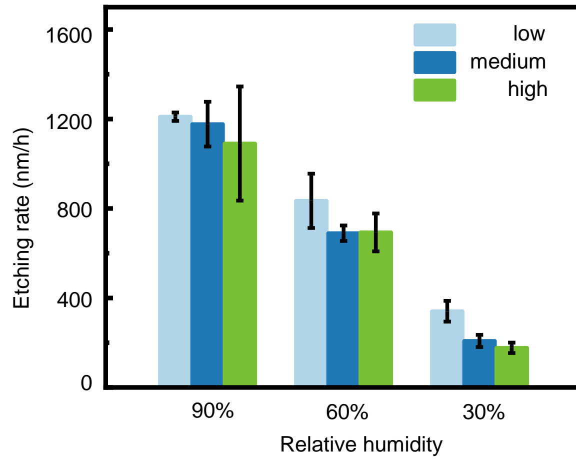


**Figure S8. Si degradation rates resulting from moisture uptake as a function of doping levels and RH at 40 $^{o}$C.**

## Table S1. Comparison of triggered degradation of Si devices.

| Initiation stimulus | Degradation mechanism | Demonstrated devices | Failure time | End product | Ref |
|---|---|---|---|---|---|
| **Laser** | Laser induces lithiation and moisture uptake triggers subsequent alkaline degradation | Si IC chips | 8 s: sever cracking of IC chips<br>5 mins: subsequent degradation into debris | Severe cracking and reactions turn Si IC chips into $Li_xSi$ and non-recoverable debris | **This work** |
| **Water** | Water-soluble substrate | COTS chips | 300 s | Dissolution of the substrate | 1 |
| **Heat** | Mechanical force | Thin CMOS chips (25 μm) | 10 s | Cracking of the top Si layer | 2 |
| | | Si-NM MOSFET arrays | 3 mins | Cracking of Si-NM MOSFET | 3 |
| | | Si-NM nMOS arrays | 62 h | Disintegration of transistor arrays | 4 |
| | | Si-NM phototransistors | 1 min | Cracking of functional layers | 5 |
| | Chemical etching | CMOS chips | 30 s | Surface etching of passivation oxide layer | 6 |
| | | NFC chips | 30 s | Erosion of the surface layer of NFC chips | 7 |
| | Nanothermite | Si wafers | 2-3 ms | Fracturing or disintegration of Si wafer | 8-9 |
| | | Porous Si wafers | 10 ms | Combustion or explosion of the porous Si layer | 10 |
| | | Si wafers | 4 ms | Shattering of wafer chips | 11 |
| | | OTS Si MEMS chips | 10-15s | Destruction of surface components | 12 |
| **Light** | UV light triggers photodegradable substrates | Si-NM MOSFET array | 230 mins | Disintegration of transistor arrays | 13 |
| **Electricity** | Electric spark ignition | OTS Si MEMS chips | 2-15 s | Etching of surface metallization | 12 |
| | Electrochemical lithiation | Si MOSFET IC chips (5 μm) | 9-12 h | $Li_xSi$ and extensive micro-scale cracks | 14 |

1. J. W. Shin *et al.*, Biologically Safe, Degradable Self-Destruction System for On-Demand, Programmable Transient Electronics. *Acs Nano* **15**, 19310-19320 (2021).

2. A. Gumus *et al.*, Expandable Polymer Enabled Wirelessly Destructible High-Performance Solid State Electronics. *Advanced Materials Technologies* **2** (2017).

3. G. Li *et al.*, High-Temperature-Triggered Thermally Degradable Electronics Based on Flexible Silicon Nanomembranes. *Advanced Functional Materials* **28** (2018).

4. B. H. Kim *et al.*, Dry Transient Electronic Systems by Use of Materials that Sublime. *Advanced Functional Materials* **27** (2017).

5. G. Li *et al.*, Flexible Transient Phototransistors by Use of Wafer-Compatible Transferred Silicon Nanomembranes. *Small* **14** (2018).

6. V. Gund *et al.* (2016) Transient micropackets for silicon dioxide and polymer-based vaporizable electronics. in *29th IEEE International Conference on Micro Electro Mechanical Systems (MEMS)* (Shanghai, PEOPLES R CHINA), pp 1153-1156.

7. C. H. Lee *et al.*, Materials and Wireless Microfluidic Systems for Electronics Capable of Chemical Dissolution on Demand. *Advanced Functional Materials* **25**, 1338-1343 (2015).

8. E. R. Westphal *et al.*, The Effects of Confinement on the Fracturing Performance of Printed Nanothermites. *Propellants Explosives Pyrotechnics* **44**, 47-54 (2019).

9. T. J. Fleck *et al.*, Controlled Substrate Destruction Using Nanothermite. *Propellants Explosives Pyrotechnics* **42**, 579-584 (2017).

10. S. K. Lazarouk, A. V. Dolbik, P. V. Jaguiro, V. A. Labunov, V. E. Borisenko, Fast exothermic processes in porous silicon. *Semiconductors* **39**, 881-883 (2005).

11. X. Ma *et al.*, Additive-Free Energetic Film Based on Graphene Oxide and Nanoscale Energetic Coordination Polymer for Transient Microchip. *Advanced Functional Materials* **31** (2021).

12. S. S. Pandey, N. Banerjee, Y. Xie, C. H. Mastrangelo, Self-Destructing Secured Microchips by On-Chip Triggered Energetic and Corrosive Attacks for Transient Electronics. *Advanced Materials Technologies* **3** (2018).

13. H. L. Hernandez *et al.*, Triggered Transience of Metastable Poly(phthalaldehyde) for Transient Electronics. *Advanced Materials* **26**, 7637-7642 (2014).

14. Y. Chen *et al.*, Electrochemically triggered degradation of silicon membranes for smart on-demand transient electronic devices. *Nanotechnology* **30** (2019).

**Movie S1. The moisture uptake process from ambient environment with normal humidity. The melting of the encapsulation layer of the fluidic reservoir is achieved using a hot plate with temperature set at 40 $^{o}$C.**

**Movie S2. Laser triggered degradation process of a Si IC chip. Laser triggers severe cracking of the IC chip (~ 8 s). Subsequent water uptake and outflow of alkaline solutions enables further thorough degradation of the IC chip into debris (~ 5 mins)**